Swine Promyelocytic Leukemia Isoform II Inhibits Pseudorabies Virus Infection by Suppressing Viral Gene Transcription in PML-NBs

Cuilian Yu,[a] Aotian Xu,[a] Yue Lang,[a] Chao Qin,[a] Xiufang Yuan,[b] Wenhai Feng,[c] Mengdong Wang,[a] Chao Gao,[a] Jinwen Chen,[a] Rui Zhang[a]# and Jun Tang [a]#

[a] College of Veterinary Medicine, China Agricultural University, Beijing, China

[b] Institute of Animal Husbandry and Veterinary Science, Zhejiang Academy of Agricultural Sciences, Hangzhou, China

[c] State Key Laboratory of Agrobiotechnology and Department of Microbiology and Immunology, College of Biological Sciences, China Agricultural University, Beijing, China

corresponding authors

Correspondence should be addressed to: Jun Tang and Rui Zhang, College of Veterinary Medicine, China Agricultural University, 2 Yuanmingyuan West Rd. Haidian district, Beijing, China, 100193. Tel: 86-(10)-6273-2328/-6273-3484; Email: jtang@cau.edu.cn and zhangrui_2046@163.com

Running Head: Swine PML-II inhibits PRV

The abstract contains 159 words, and the text contains 5010 words.

ABSTRACT

Promyelocytic leukaemia nuclear bodies (PML-NBs) possess an important intrinsic antiviral activity against α-herpesvirus infection. PML is the structural backbone of NBs, comprising different isoforms. However, the contribution of each isoform to α-herpesvirus restriction is not well understood. Here, we report the role of PML-NBs and swine PML (sPML) isoforms in pseudorabies virus (PRV) infection in its natural host swine cells. We found that sPML-NBs exhibit an anti-PRV activity in the context of increasing the expression level of endogenous sPML. Of four sPML isoforms cloned and examined, only isoform sPML-II/IIa, not sPML-I and IVa, expressed in a sPML knockout cells inhibits PRV infection. Both the unique 7b region of sPML-II and sumoylation-dependent normal formation of PML-NBs are required. 7b possesses a transcriptional repression activity and suppresses viral gene transcription during PRV infection with the cysteine residue 589 and 599 being critically involved. We conclude that sPML-NBs inhibit PRV infection by repressing viral gene transcription through the 7b region of sPML-II.

IMPORTANCE

PML-NBs are nuclear sites that mediate the antiviral restriction of α-herpesvirus gene expression and replication. However, the contrition of each PML isoform to this activity of PML-NBs is not well characterized. Using PRV and its natural host swine cells as a system, we have discovered that the unique C-terminus of sPML

42 isoform II is required for PML-NBs to inhibit PRV infection by directly engaging in
43 repression of viral gene transcription. Our study not only confirms in swine cells
44 that PML-NBs have an anti-viral function, but also presents a mechanism to
45 suggest that PML-NBs inhibit viral infection in an isoform specific manner.

INTRODUCTION

Promyelocytic leukaemia nuclear bodies (PML-NBs) is a PML protein-based sub-nuclear structure with an intrinsic anti-viral activity against a wide range of RNA and DNA viruses. More than 150 proteins have been identified either transiently or residentially associated with PML-NBs, many of which possesses an anti-viral activity including Sp100, Daxx, ATRX, HIRA and MORC3 (1-7). As a countermeasure, numerous viruses have evolved strategies to disrupt or degrade PML-NBs underscoring the importance of this structure in cellular anti-viral defense. In the case of α-herpesvirus HSV-1, PML is ubiquitinated and degraded by the viral E3 ubiquitin ligase ICP0 (8). Thus, an ICP0-deleted HSV-1 mutant is often used to study the role of PML-NBs in HSV-1 restriction.

PML-NBs are involved in multiple mechanisms to restrict herpesvirus infection. It has been long known that PML-NBs have a complex and intimate relationship with herpesvirus DNAs. Recent studies have shown that in addition to immediately entrapping a HSV-1 viral genome after nuclear entry and blocking its replication, PML-NBs are also recruited to the sites of progeny viral DNAs by the nuclear DNA sensor IFI16, and contribute to the repression of viral gene transcription (9-11). The involvement of PML-NBs in this process concerns PML-NBs associated proteins. For example, Daxx and ATRX are critically involved in an epigenetically silencing mechanism (1, 5, 12, 13). However, it is not clear whether PML protein

66 plays a direct role in transcription repression in addition to the recruitment of other
67 proteins. In addition, PML-NBs are also engaged in eliciting innate immune
68 responsive gene transcription, as well as the sequestration of a viral capsid protein
69 to restrict virus infection (14-17).

70 PML is the structural component of PML-NBs, which belongs to the tripartite
71 motif family with a characteristic RBCC region that includes a RING domain, two
72 B boxes and a coiled-coil (CC) region (18, 19). Due to alternative splicing of
73 mRNAs, a single *PML* gene generates six major nuclear isoforms, referred as
74 PML-I to PML-VI in human cells. These isoforms share a common N-terminal
75 region (exon 1 to 6) containing the RBCC motif (exon 2 to 3), but differ in their C-
76 termini (18, 20, 21). Derivatives of each isoform lacking exon 5 (referred as a) or
77 exon 5 and 6 (referred as b) or exon 4, 5 and 6 (referred as c) might also exist (18,
78 20). Increasing evidence indicate the unique C-terminal region of each isoform
79 contributes greatly to the composition and functionality of PML-NBs (15, 20, 22,
80 23), however, the exact role of each isoform remains poorly understood. In the
81 context of anti-herpesvirus defense, it has been reported that in varicella-zoster
82 virus (VZV) infection only PML-IV sequesters the capsid protein encoded by
83 ORF23 leading to VZV restriction (16), whereas in HSV-1 infection PML-I and
84 PML-II play a major role with an unknown mechanism (24).

85 Herpesvirus infection is considered to be species specific in general, which is

partly as a result of long-term co-evolution between viruses and host species. However, the relationship between herpesvirus infection and PML-NBs are mostly characterized in human cells. Given the complexity of PML isoforms and their differential role in VZV and HSV-1 infection in human cells, we hypothesize that PML-NBs in other species might also evolve a specialized function targeting their natural herpesviruses in an isoform specific manner. In this study, we have explored PML-NBs in swine cells in relation to pseudorabies virus (PRV) infection, particularly the role of swine PML (sPML) isoform in restricting PRV infection, and found that sPML-NBs inhibits PRV infection in a sPML-II dependent manner.

PRV is a swine α-herpesvirus which can cause Aujeszky's disease characterized by respiratory distress, nervous disorder and reproductive failure (25). It is often used as a complement model to study the life-cycle and pathogenicity of alpha-herpesvirus subfamily. As with HSV-1, PRV infection in human cells results in disappearance of PML-NBs. EP0, the PRV ortholog of ICP0, degrades PML in human cells (26, 27). However, the relationship between PRV infection and PML-NBs in its natural host swine cells has not been characterized. In this study, we found that PML-NBs in swine cells were disrupted during PRV infection and that the anti-PRV activity of sPML-NBs may depend on the expression level of sPML. Of four sPML isoforms cloned and examined, only isoform II/IIa which contain exon 7b restrict PRV infection. Exon 7b has an ability

106 to repress viral gene transcriptions with cysteine residues in a ring-like region being

107 critically involved.

MATERIALS AND METHODS

Cell culture and viruses

HEK293T cells (human embryonic kidney, ATCC #CRL-3216), PK15 cells (porcine kidney cells, ATCC #CCL-33), Vero cells (ATCC #CCL-81) and CRL cells (porcine alveolar macrophage cells) were cultured in Dulbecco's modified Eagle's medium (DMEM). Primary porcine alveolar macrophages (PAM) cells were obtained by lavaging the lungs of 6–8-wk-old specific pathogen–free (SPF) pigs, as described previously (28), and maintained in RPMI 1640. The primary porcine kidney cells were harvested from the kidneys of 21 day-old specific pathogen–free (SPF) piglets, as described previously (29), and maintained in DMEM. All cells were cultured in medium supplemented with 10% (v/v) FBS and maintained in a humidified incubator with 5% CO2 at 37℃.

PRV WT (Bartha K61), the recombinant PRV EP0-Knockout virus (PRV-EP0 KO) and KOS strain of HSV-1 were described previously (30, 31).

Reagents

Anti-GFP (SC-9996) antibody was purchased from Santa Cruz Biotechnology (Santa Cruz, CA, USA). FLAG (M2 F-1804) antibodies, Triton X-100 and N-ethylmaleimide (NEM) were purchased from Sigma (St Louis, MO, USA). Anti-α-Tubulin mAb PM054 was purchased from MBL. DAPI (4,6-diamidino-2-

phenylindole) was purchased from Beyotime Institute of Biotechnology. The antibodies against PRV TK, PRV US3, PRV EP0 were described previously (30, 32, 33). Mouse polyclonal antibodies against PRV IE180, VP5 and gD were raised in mice individually with the 1-666aa, 710-1280aa, 240-400aa region of each protein as antigens. Rabbit polyclonal antibodies against swine PML were described previously (33). Sodium dodecyl sulfate (SDS) was purchased from Scientific Research Ievei. DL-Dithiothreitol (DTT) and bovine serum albumin fraction (BSA) were purchased from Amresco Biotechnology. Puromycin and polybrene were also purchased from Amresco. Swine IFNα (sIFNα) was described previously (33).

Plasmids and transfection

sPML-I, -II, -IIa and -IVa cDNAs were amplified by PCR using cDNAs made from sIFNα-stimulated PK15 cells as templates and then cloned into Flag-/pRK5, Flag-/pSin-EF2-puro and Flag-GFP-/pSin-EF2-puro vector. All the mutants including deletions, point mutations and fusions were generated by PCR and cloned into Flag-/pRK5 or pSin-EF2-puro vector or both. 7b-nls was created by fusing the NLS sequence of 5'-PKKKRKV-3' to the C-terminus of 7b. Gal-/pRK5, 5xGal-TK-luciferase reporter and pCMV-β-galactosidase plasmid were previously described (34). All the constructs were confirmed by DNA sequencing.

List of PCR and mutagenic primer is provided in Table 1.

Plasmids were transfected into HEK293T cells using jetPRIME (Polyplus) and PK15 cells using Lipofectamine LTX Reagent (Invitrogen) following the corresponding manufacturer's protocol.

Generation of sPML-KO PK15 cells

sPML-KO PK15 cells were generated using TALEN technology using the Fast TALE™ TALEN Assembly Kit (SIDANSAI) according to the manufacturer's instruction (35). The first exon of PML was targeted by TALEN with the left and right arm sequence of being -GCAGCAGGAACCGGCAC- and -GGGGTCGTCTTGGGGCA-, respectively. PK15 cells were seeded into a 6-well dish and transfected with TALEN plasmids when 70% confluency was achieved. After 24 h of transfection, a medium contained 2.5 μg/ml puromycin was added to the cells. 72 h later, the survived cells were diluted and seeded into a 96-well dish at 0.5 cell/well in a complete DMEM medium. Cells of a single colony were expanded and then examined for sPML expression by immunofluorescent microscopy. sPML-NBs negative cells were further subject to sequencing of exon-1 for verification.

Generation of stable cell lines

pSin-EF2-puro plasmids encoding aPML-I to -IVa or mutants were transfected into HEK293 cells together with two lentivirus packaging plasmids, pMD2.G, and psPAX2, and the ratio of pSin: psPAX2: pMD2.G was 2:2:1. After 48 h of

transfection, the supernatants were harvested, filtered through a 0.45 u syringe filter and then used to infect sPML-WT or sPML-KO PK15 cells in the presence of 8 μg/mL of polybrene. Cells stably expressing sPML isoforms or mutants were selected by treating the infected cells with puromycin at 5 μg/mL for a week.

Immunofluorescence microscopy.

Cells grown on glass coverslips were fixed in 4% paraformaldehyde for 30 min at room temperature and then permeabilized with 0.2% Triton X-100 for 15 min on ice. After washing and blocking in phosphate-buffered saline (PBS) containing 1% bovine serum albumin (BSA) for 30 min, the cells were incubated with specific primary antibodies for 1 h at room temperature followed by FITC or TRITC conjugated secondary antibodies for 30 min. Nuclei were stained with DAPI for 3 to 5 min. Images were captured using a Nikon Eclipse Ni-E microscope or a Leica Wetzlar GmbH microscope. The captured images were processed and analyzed using SPOT software (Nikon).

Western blot analysis

Whole-cell lysates were prepared in lysis buffer (50 mM Tris-Cl at pH 8.0, 150 mM NaCl, 1.0% Triton X-100, 10% glycerol, 20 mM NaF, 1 mM DTT, and 1× complete protease mixture). The proteins were separated by 10% sodium dodecyl sulfate-polyacrylamide gel electrophoresis (SDS-PAGE) and transferred to nitrocellulose membranes. The membranes were blocked with 5% skim milk in PBST (PBS

187 containing 0.5% Tween 20) for 2 h at room temperature and were then incubated
188 with specific primary antibodies overnight at 4°C followed by secondary antibodies
189 for 45 min at room temperature. The reactive protein bands were visualized using
190 an enhanced chemiluminescence (ECL) reagent with Tanon-5200 luminescent
191 imaging workstation.

192 **Virus infection and titer determination**

193 PK15 cells were infected with PRV WT or PRV-EP0 KO viruses with the indicated
194 MOI for 1 h followed by washes with PBS and incubation in complete DMEM
195 supplemented with 5% FBS for the indicated durations. The supernatants were
196 collected for titer determination and the remaining cells were used for western blot
197 analysis.

198 The viral yields of PRV WT or PRV-EP0 KO were determined by plaque assay
199 in Vero cells. Briefly, the collected supernatants from viruses infected PK15 cells
200 were cleared of cell debris by centrifugation, and then used to infect Vero cells in
201 duplicate or triplicate with serial dilutions for 1 h in serum free DMEM. After washes
202 with PBS, the cells were overlaid with 1× DMEM/1% agarose, and incubated at
203 37℃ until plaque formation was observed (72 h-96 h). The cells were stained with
204 0.5% neutral red for 4 h-6 h at 37℃, and the plaques were counted.

205 **Real-time PCR**

206 Total RNAs were extracted from PK15 cells using TRIzol (Invitrogen) following the

manufacturer's protocol. A total of 0.8 μg RNA from different treatments was reversely transcribed into cDNA using M-MLV reverse transcriptase (Promega) with an oligo (dT) 18 primer. Real-time PCR was performed using an UltraSYBR Mixture (Beijing CoWin Biotech, Beijing, China) on a ViiA 7 real-time PCR system (Applied Biosystems). Viral rRNAs were normalized to swine 28S rRNA expression. Gene-specific primers used for RT–PCR assays included PRV-IE180 forward (5'-ACCACCACCGTCGCCGTCGAGACCGTC-3') and reverse (5'-GACGGTCTCGACGGCGACGGTGGTGGT-3'), PRV-TK forward (5'-ATGACGGTCGTCTTTGACCGCCAC-3') and reverse (5'-CGCTGATGTCCCCGACGATGAA-3'), PRV-EP0 forward (5'-GGGTGTGAACTATATCGACACGTC-3') and reverse (5'-TCAGAGTCAGAGTGTGCCTCG-3') and swine 28S forward (5'-GGGCCGAAACGATCTCAACC-3') and reverse (5'-GCCGGGCTTCTTACCCATT-3') primers.

Reporter Assay

HEK293T cells were seeded in 24-well plates and transfected with 0.4 μg of 5xGal-TK-luciferase reporter gene plasmid, 50 ng of pCMV-β-galactosidase, and various amounts of plasmids expressing Gal, Gal-7b, Gal-7b(2CA) or Flag-7b. The total amount of DNA was made constant by adding the pRK5 vector. 24 h after transfection, cells were harvested and assayed for luciferase activity with a firefly

227 luciferase system (Promega), according to the manufacturer's instruction.
228 Luciferase activities were normalized on the basis of the activities of the co-
229 transfected β-galactosidase. Data shown are representative of three independent
230 experiments done in duplicate.

231 **Statistical analysis**

232 Statistical analyses were performed using GraphPad Prism software to perform
233 Student's t test or analysis of variance (ANOVA) on at least three independent
234 replicates. P values of <0.05 were considered statistically significant for each test.
235 * $P < 0.05$; ** $P < 0.01$; *** $P < 0.001$.

RESULTS

Swine PML-NBs inhibit PRV

To characterize the relationship between PML-NBs and PRV in porcine cells, we first observed sPML-NBs in several types of porcine cells by performing immunofluorescent microscopy using an antibody against sPML. sPML forms NBs as expected in all the cell types examined, and the number of sPML-NBs in freshly isolated primary cells including porcine kidney cells and porcine alveolar macrophages (PAM) was substantially higher than the established cell lines PK15 and CRL (Fig. 1A left and middle panels). This result is consistent with the reported findings that the number of PML-NBs is low in immortalized or certain types of cancer cells due to aberrant signaling in these cells leading to PML destabilization (36, 37). The low number of sPML-NBs in PK15 and CRL cells was dramatically increased by interferon treatment for 12 h (Fig. 1A right panel), indicating that *spml* is also an interferon responsive gene.

We then examined the effect of PRV infection on sPML-NBs by infecting cells with PRV for 24 h. PRV infection resulted in disappearance of sPML-NBs in primary porcine kidney cells or PK15 and CRL cells pre-treated with swine IFNa (Fig. 1B), confirming in porcine cells that a-herpesvirus infection disrupts PML-NBs.

Next, we analyzed the effect of knockout of sPML in PK15 cells on PRV infection. sPML was knocked out in PK15 cells by using TALEN technique.

Consequently, no sPML fluorescent signal was detected in sPML-knockout (sPML-KO) cells even after interferon treatment (Fig. 1C). sPML-WT and -KO PK15 cells with or without IFN pretreatment were infected with a PRV Bartha wild type (WT) and an EP0 deleted strain (EP0 KO) at MOI 0.1 and then examined viral gene expression by western blotting or infectious viral particle production by measuring the PFU (Fig. 1D and 1E). EP0 is a homolog of ICP0 of HSV-1 known to disrupt PML-NBs (26, 27). When not treated with sIFNa, no significant difference in viral replication for both WT and EP0 KO PRV strains were observed between these two cell lines. These results were not surprising given that the number of sPML-NBs in PK15 cells is remarkably low. Pre-treatment of cells with IFN significantly increased the number of sPML-NBs, and also markedly reduced replications of WT and EP0 KO PRV in PK15 WT cells. IFN also reduced viral replications in sPML-KO cells, but the effects were much less dramatic, indicating that sPML contributed to the anti-viral effect of IFN. Compared with the PRV-WT, EP0 KO viruses were more sensitive to IFN in both cell lines, confirming the previous findings that EP0 is a prominent viral protein that disrupts cellular anti-viral mechanisms such as PML-NBs.

sPML isoform II and IIa not I and IVa possess an anti-PRV activity

To validate the anti-viral activity of sPML to PRV, we set out to examine the direct effect of expressing sPML on PRV infection by first cloning sPML cDNAs. Analysis

of the human and swine *pml* gene indicates *spml* is very similar to human *pml* in terms to exon composition and alternative splicing sites (Fig. 2A), thus, likely generates similar isoforms to those identified in human. Based on the predicated cDNA sequences for the main nuclear sPML isoforms, we successfully cloned four sPML isoforms in this study through PCR using the cDNAs generated from PK15 cells as templates, and designated them as sPML-I, sPML-II, sPML-IIa and sPML-IVa corresponding to each related human PML isoform. sPML-IIa and -IVa are variants of sPML-II and IV, respectively, lacking exon 5 (Fig. 2A). All four sPML isoforms formed typical PML-NBs when expressed in sPML-KO PK15 cells (Fig. 2B).

We then examined whether expressing each sPML isoform in PK15 cells inhibited PRV infection. sPML-KO PK15 cells stably expressing each GFP-sPML isoform as well as GFP were individually established by lentiviral transduction and selection, and the infectivity of these cells to both PRV-WT and -EP0 KO was compared by western analysis of viral protein expressions and viral titer measurements (Fig. 2C and 2D). Compared to GFP expressing cells, sPML-II and -IIa inhibited PRV infections, and to a much more significant degree PRV-EP0 KO infections, whereas sPML-I and -IVa, showed much weaker or even no inhibitions. The similar result was confirmed when F-sPML isoforms were transiently expressed in PK15 cells followed by virus infections (Fig. 2E, 2F, 2G and 2H).

296 Overall, these data suggest that despite all 4 isoforms forming typical PML-
297 NBs, only sPML-II and –IIa showed strong anti-PRV activity, particularly to PRV-
298 EP0 KO strain. PRV-EP0 KO strain was thus used for most of subsequent studies.

299 **The unique C-terminal region encoded by exon 7b of sPML-II and -IIa is**
300 **required for sPML to inhibit PRV infection**

301 As sPML-II and –IIa carry a unique exon 7b region, we asked whether this region
302 possesses an anti-PRV activity. We deleted 7b from F-sPML-II and –IIa (Δ7b), and
303 also constructed a plasmid only expressing 7b region fused with a NLS C-
304 terminally (7b-nls) (Fig. 3A). Adding nls is to ensure 7b is able to enter the nucleus.
305 The anti-PRV activities of these mutants were then analyzed by transfecting the
306 plasmids into PK15 cells followed by PRV-EP0 KO infections. Western blot
307 analysis and viral titer measurements showed that F-sPML-IIΔ7b and –IIaΔ7b
308 completely lost the anti-PRV activity, whereas 7b-nls still strongly inhibited PRV
309 infection, similar to PML-II and -IIa (Fig. 3B and 3C). Additionally, 7b fused to the
310 C-terminal end of GFP-sPML-I (GFP-sPML-I-7b), an isoform without an anti-PRV
311 activity, made the isoform gain the ability to inhibit PRV infection (Fig. 3D, 3E and
312 3F). This was demonstrated in sPML-KO PK15 cells stably expressing GFP, GFP-
313 sPML-I or GFP-sPML-I-7b. Collectively, these data indicate that 7b possesses an
314 anti-PRV activity, which gives sPML-II/IIa the ability to inhibit PRV infection.

315 **Cysteine residue 589 and 599 in 7b is critically involved in the anti-PRV**

316 **activity of 7b and sPML-II/IIa**

317 To gain more insight into the structural requirement of 7b to inhibit PRV, we
318 analyzed 7b using SMART(38) and revealed that the region of 585-610aa in sPML-
319 II might have a possibility to form a C3H1 type finger despite only two cysteine
320 residues 589 and 599 present (Fig. 4A). To examine whether these two cysteines
321 are involved in the anti-PRV activity of 7b and sPML-II, we mutated them
322 simultaneously or individually into alanine (s) in 7b or sPML-II (Fig. 4A). We then
323 examined the anti-PRV activity of 7b mutants upon transient (Fig. 4B and 4C) and
324 stable expression (Fig. 4D) in PK15 WT cells, and that of sPML-II mutants upon
325 stable expression in sPML-KO PK15 cells (Fig. 4E). Mutation of both cysteines
326 (2CA) or either one (C589A or C599A) completely abolished the anti-PRV activity
327 of 7b or sPML-II (Fig. 4B, 4C, 4D and 4E). These results indicate that cysteine 589
328 and 599 in 7b is critically involved in the anti-PRV activity of 7b and sPML-II/IIa.

329 **Localization of 7b in sPML-NB is required for 7b to inhibit PRV infection**

330 The result that expression of just the 7b portion of PML-II in PK15 displays a strong
331 anti-PRV activity is intriguing, raising a question whether formation of sPML-NBs
332 is required for a sPML protein to perform its anti-PRV activity. Since the
333 aforementioned experiments were performed in sPML wild type PK15 cells, we
334 asked whether endogenous sPML-NBs is involved in 7b mediated anti-PRV activity.
335 To test this, we stably expressed F-7b-nls in both sPML-WT and -KO PK15 cells

by simultaneously performing lentiviral transductions and selections, and then compared the anti-PRV effect of F-7b-nls in both cell lines, with empty vector and F-7b (2CA)-nls as controls (Fig. 5A, 5B, 5C and 5D). F-7b only exhibited anti-PRV activity in sPML-WT PK15 cells (Fig. 5A and 5B) but no in sPML-KO PK15 (Fig.5C and 5D), suggesting that endogenous sPML-NBs may play a role in facilitating 7b to implement its anti-PRV function. As expected, F-7b(2CA) did not show any inhibition in both cell lines.

To further investigate the connection between sPML-NBs and 7b, we immunostained F-7b in sPML-WT and -KO cells stably expressing F-7b-nls. Confocal microscopy analysis revealed that a portion of F-7b-nls in sPML-WT cells localized in nuclear dot structures, which proved to be sPML-NBs by co-staining with an anti-sPML antibody (Fig. 5E upper panel). In contrast, F-7b-nls in sPML-KO cells was completely diffused in the nucleus (Fig. 5E lower panel). These data suggest that 7b can be recruited into sPML-NBs, and this recruitment may be critical for 7b to execute its anti-PRV function. Supportively, overexpression of F-7b without NLS in sPML-WT PK15 cells, which mainly localized in the cytoplasm, did not show any anti-PRV effect (Fig. 5F and 5G).

Collectively, these data suggest that a functional 7b localizing in sPML-NBs may be required for 7b to perform its anti-PRV function, and endogenous PML-NBs have the ability to recruit it.

Normal formation of sPML-II NBs is required for sPML-II to inhibit PRV

Next we asked if proper formation of PML-NBs is required for sPML-II to inhibit PRV. PML-NB assembly is initiated by PML N-terminal RBCC region mediated oligomerization, followed by RING domain dependent PML sumoylation, which mainly occurs on sites K65, 160 and 490 (39-41). PML sumoylation critically controls the maturation of PML-NBs (40, 42, 43). We thus examined if abrogation of sPML-II sumoylation affected its anti-PRV activity by either disrupting sPML-II RING or mutating its presumed major sumoylation sites K65, K160 and K482 into arginine. Analysis of the anti-PRV activity of the mutants stably expressed in sPML-KO PK15 cells in comparison with wild type sPML-II showed that the RING inactivation mutant F-sPML-II-RINGca, in which seven cysteine residues of the classic C3HC4 RING finger domain (C57/C60/C72/C77/C80/C88/C91) was mutated into alanine, lost the anti-PRV activity (Fig. 6A). Similarly, sumoylation site mutants sPML-II 2KR (K65/160R) and sPML-II 3KR (K65/160/482R) also lost the anti-PRV activity (Fig. 6C).

As expected, the upper modified bands in F-sPML-II expressing cells, which presumably were sumoylated F-sPML-II, disappeared in F-sPML-II-RINGca expressing cells (Fig. 6A), supporting that the RING finger domain critically controls PML sumoylation. However, immunostaining showed that F-sPML-II-RINGca still formed some nuclear dots even though displaying more diffused

staining in the nucleoplasm compared with wild type F-sPML-II (Fig. 6B). sPML-II 2KR and 3KR also formed some nuclear dots, but the number was greatly reduced (Fig. 6D). The nuclear dots formed by sPML-II-RINGca, 2KR and 3KR are likely aberrant sPML-NBs (Fig. 6B and 6D). sPML-II 3KR also showed cytoplasmic staining, which is probably due to a defect in nuclear translocation resulted from K482 mutation, which lies in the nuclear localization sequence of sPML 468-482aa, like K490 in human. Intriguingly, sPML-2 2KR and 3KR were difficult to detect by western analysis despite showing normal intensity of immunofluorescent staining (Fig. 6C and 6D).

Altogether, these data show that the normal formation of PML-NBs is required for sPML-II to inhibit PRV infection with PML sumoylation being critically involved. Aberrant sPML-NBs formed by sPML-II due to RING or sumoylation site mutations lost the anti-PRV activity despite the presence of 7b.

sPML exon 7b inhibits viral gene transcriptions

To explore the mechanism underlying PRV inhibition by sPML-II, we focused on 7b and its role in viral gene transcription because it is the effector region of sPML-II which may possess a putative ring-like structure (44). PK15 cells transfected with EV, F-7b-nls or -7b (2CA)-nls were infected with a high titer of PRV (MOI=5), and the kinetics of PRV viral protein expressions (Fig. 7A) and gene transcriptions (Fig. 7B) were monitored at 2, 4 and 6 hours post-infection (hpi). Western analysis

revealed that compared with control cells, viral protein expressions in 7b, but not 7b (2CA), expressing cells were substantially reduced from the time point when detection of these proteins became evident, which was 4 hpi for the immediate early gene IE180 and the early gene (E) US3, and 6 hpi for the late gene gD (Fig. 7A). Viral mRNA measurements indicated relative to the control cells the transcriptions of IE180 and two E genes (EP0 and TK) in 7b expressing cells were also significantly reduced from an earlier time point (2 hpi) when we began to monitor viral mRNA productions (Fig. 7B). These results suggest 7b is clearly involved in transcriptional repression of IE180, and it may also inhibit the transcriptions of other viral genes. However, because the expression of IE180 affects later viral gene transcriptions (25), we cannot rule out the possibility that lower expressions of E and L genes in 7b expressing cells is due to the initial lower IE180 expression in 7b expressing cells. Nevertheless, these results suggest 7b may be involved in inhibition of viral gene transcriptions, particularly IE180.

To direct determine whether 7b possesses a transcriptional repression activity, we fused 7b or 7b (2CA) to the Gal4 DNA-binding domain (Gal-7b or Gal-7b(2CA)) and introduced this fusion into 293T cells together with a luciferase reporter plasmid containing five Gal4 DNA-binding sites upstream of the thymidine kinase (TK) promoter. Gal-7b but not the Gal-7b (2CA) strongly inhibited the luciferase activity (Fig. 7C) and in a dose-dependent manner (Fig. 7D). This transcription

repression was dependent on the targeting of 7b to the promoter, as Flag-7b-nls failed to inhibit luciferase activity (Fig. 7C). Thus, exon 7b can function as a transcription repressor when tethered to a promoter.

DISCUSSION

Here, we demonstrated in swine cells that sPML-NBs inhibit PRV infection in an isoform specific manner. We revealed that only sPML-II/-IIa which carry the unique 7b region can inhibit PRV infection, and that 7b possesses transcriptional repression activity that can suppress viral gene transcriptions at normal sPML-NBs. Our studies not only characterized sPML-NBs in relation to PRV infection for the first time, but also provide a mechanism to explain how sPML-NBs inhibit PRV infection in a sPML-II dependent fashion, which we believe can be extended to explain other scenarios of viral inhibition by a PML isoform.

Our findings suggest that sPML-NBs require at least two properties to inhibit PRV infections: one is the formation of a normal PML-NB with an ability to recruit other molecular, which is RBCC- and sumoylation-dependent; the other is 7b mediated transcriptional repression, which can be provided either as a part of a sPML molecule or by trans. The formation of a functional NB per se is not sufficient but necessary to inhibit PRV infection. sPML molecules with a property to form normal NBs but without a functional 7b element fail to efficiently restrict PRV. These sPML molecules include sPML-I and -IVa, as well sPML-II mutants with either 7b deleted (Δ7b) or transcriptional repression activity abolished (C589A, C599A and

437 2CA). On the other hand, RING or major sumoylation defective sPML-II mutants
438 also fail to inhibit PRV despite having a functional 7b. Moreover, 7b can only exert
439 its anti-PRV function on the condition of localizing in a functional sPML-NB either
440 as a part of sPML-II, fused with sPML-I or even being recruited there as a
441 separated molecule. These data strongly argue that both normal PML-NBs
442 formation and 7b moiety are required to enable a sPML isoform to restrict PRV
443 infection.

444 Suppression of viral gene transcription is a critical cellular anti-viral
445 mechanism. It has been reported that numerous proteins are targeted to the HSV-
446 1 viral genome and act coordinately to inhibit viral DNA replication and gene
447 transcription (1, 45, 46). PML-NBs concentrated a number of molecules involved
448 in viral suppression are also recruited to HSV-1 viral DNAs by ATRX or nuclear
449 DNA sensor IFI16 (10, 11, 13). This recruitment process requires a functional
450 RBCC region, PML sumoylation and a SIM motif. In addition to accumulating anti-
451 viral proteins to a viral genome, PML-NBs may also promote various anti-viral
452 processes as a result of multiple dynamic SUMO-SIM interactions, for example
453 Daxx and ATRX meditated epigenetic silencing of viral genomes (2, 5, 47). We
454 speculate that the similar scenario may also exist in swine cells in which sPML-
455 NBs are recruited to PRV genomes allowing the 7b moiety to repress viral gene
456 transcriptions and at the same time promote this process. The observation that 7b

457 can form nuclear dots only in cells with endogenous PML which co-localize with
458 PML-NBs indicates that 7b may also interact with certain component(s) of PML-
459 NBs. Nevertheless, an important contribution of PML-NBs moiety to a-herpesvirus
460 restriction is to recruit gene transcription repressors to viral genomes, and some
461 of the repressors are certain PML isoforms.

462 sPML-II plays a direct role in repressing PRV gene transcriptions. PML
463 proteins are unique in a sense that splicing variants of all isoforms reportedly co-
464 exist in a NB (36). Increasing evidence indicate that the unique C-terminal moiety
465 of each PML isoform contributes greatly to the formation and diverse functions of
466 PML-NBs. For instance, PML-IV has been extensively studied in the field of cancer
467 biology due to its unique role in binding and regulating the tumor suppressor p53
468 (48, 49). In the case of HSV-1 infection, only PML-I and -II are reported to partially
469 mediate the anti-HSV-1 functions of PML-NBs, indicating the C-terminal regions of
470 these two isoforms are involved in HSV-1 restriction (24), although the
471 mechanisms by which PML-I and -II suppress HSV-I are not known. We provide
472 evidence to suggest that the mechanism for sPML-II to restrict PRV is to repress
473 viral gene transcriptions mediated by the 7b region. In the presence of 7b, the
474 transcriptions and expressions of all the viral genes examined were suppressed
475 and 7b directly inhibits a reporter gene transcription when tethered to its promoter.
476 Interestingly, homology analysis indicates the c-terminus of PML-I is very

conserved between human and swine sharing 74% identity, whereas PML-II 7b is relatively diverse with only 46% identity. Thus, the mechanism by which PML-I and -II restrict HSV-1 might be different from that of sPML-II inhibiting PRV. More comparative studies are required to distinguish the virus specific function of PML isoforms verses the general antiviral property of PML-NBs.

We don't know the exact mechanism by which 7b inhibits gene transcriptions, but have identified two cysteine residues in a putative zinc finger-like region critically involved in this process. Mutation of either residue resulted in 7b and sPML-II losing the ability to suppress gene transcriptions and/or restrict PRV infection. Although based on the predication the likelihood for the putative zinc finger-like region to form a zinc finger is low, these two cysteine residues certainly play an important role structurally.

ACKNOWLEDGMENTS

This work was supported by the National Key Research and Development Program of China (grant 2016YFD0500100) and the National Natural Science Foundation of China (grant 31500703).

REFERENCES

1. **Full F, Ensser A.** 2019. Early Nuclear Events after Herpesviral Infection. J Clin Med **8**.

2. **Everett RD, Murray J.** 2005. ND10 components relocate to sites associated with herpes simplex virus type 1 nucleoprotein complexes during virus infection. J Virol **79:**5078-5089.

3. **Isaac A, Wilcox KW, Taylor JL.** 2006. SP100B, a repressor of gene expression preferentially binds to DNA with unmethylated CpGs. J Cell Biochem **98:**1106-1122.

4. **Schreiner S, Burck C, Glass M, Groitl P, Wimmer P, Kinkley S, Mund A, Everett RD, Dobner T.** 2013. Control of human adenovirus type 5 gene expression by cellular Daxx/ATRX chromatin-associated complexes. Nucleic Acids Res **41:**3532-3550.

5. **Cabral JM, Oh HS, Knipe DM.** 2018. ATRX promotes maintenance of herpes simplex virus heterochromatin during chromatin stress. Elife **7**.

6. **Rai TS, Glass M, Cole JJ, Rather MI, Marsden M, Neilson M, Brock C, Humphreys IR, Everett RD, Adams PD.** 2017. Histone chaperone HIRA deposits histone H3.3 onto foreign viral DNA and contributes to anti-viral intrinsic immunity. Nucleic Acids Res **45:**11673-11683.

7. **Sloan E, Orr A, Everett RD.** 2016. MORC3, a Component of PML Nuclear

513 Bodies, Has a Role in Restricting Herpes Simplex Virus 1 and Human
514 Cytomegalovirus. J Virol **90:**8621-8633.

515 8. **Boutell C, Cuchet-Lourenco D, Vanni E, Orr A, Glass M, McFarlane S,**
516 **Everett RD.** 2011. A viral ubiquitin ligase has substrate preferential SUMO
517 targeted ubiquitin ligase activity that counteracts intrinsic antiviral defence.
518 PLoS Pathog **7:**e1002245.

519 9. **Cuchet-Lourenco D, Anderson G, Sloan E, Orr A, Everett RD.** 2013. The
520 viral ubiquitin ligase ICP0 is neither sufficient nor necessary for degradation
521 of the cellular DNA sensor IFI16 during herpes simplex virus 1 infection. J
522 Virol **87:**13422-13432.

523 10. **Everett RD.** 2016. Dynamic Response of IFI16 and Promyelocytic
524 Leukemia Nuclear Body Components to Herpes Simplex Virus 1 Infection.
525 J Virol **90:**167-179.

526 11. **Diner BA, Lum KK, Toettcher JE, Cristea IM.** 2016. Viral DNA Sensors
527 IFI16 and Cyclic GMP-AMP Synthase Possess Distinct Functions in
528 Regulating Viral Gene Expression, Immune Defenses, and Apoptotic
529 Responses during Herpesvirus Infection. mBio **7**.

530 12. **Tavalai N, Stamminger T.** 2009. Interplay between Herpesvirus Infection
531 and Host Defense by PML Nuclear Bodies. Viruses **1:**1240-1264.

532 13. **Alandijany T, Roberts APE, Conn KL, Loney C, McFarlane S, Orr A,**

Boutell C. 2018. Distinct temporal roles for the promyelocytic leukaemia (PML) protein in the sequential regulation of intracellular host immunity to HSV-1 infection. PLoS Pathog **14:**e1006769.

14. **McFarlane S, Orr A, Roberts APE, Conn KL, Iliev V, Loney C, da Silva Filipe A, Smollett K, Gu Q, Robertson N, Adams PD, Rai TS, Boutell C.** 2019. The histone chaperone HIRA promotes the induction of host innate immune defences in response to HSV-1 infection. PLoS Pathog **15:**e1007667.

15. **El Asmi F, Maroui MA, Dutrieux J, Blondel D, Nisole S, Chelbi-Alix MK.** 2014. Implication of PMLIV in both intrinsic and innate immunity. PLoS Pathog **10:**e1003975.

16. **Reichelt M, Wang L, Sommer M, Perrino J, Nour AM, Sen N, Baiker A, Zerboni L, Arvin AM.** 2011. Entrapment of viral capsids in nuclear PML cages is an intrinsic antiviral host defense against varicella-zoster virus. PLoS Pathog **7:**e1001266.

17. **Kim YE, Ahn JH.** 2015. Positive role of promyelocytic leukemia protein in type I interferon response and its regulation by human cytomegalovirus. PLoS Pathog **11:**e1004785.

18. **Jensen K, Shiels C, Freemont PS.** 2001. PML protein isoforms and the RBCC/TRIM motif. Oncogene **20:**7223-7233.

19. **Reymond A, Meroni G, Fantozzi A, Merla G, Cairo S, Luzi L, Riganelli D, Zanaria E, Messali S, Cainarca S, Guffanti A, Minucci S, Pelicci PG, Ballabio A.** 2001. The tripartite motif family identifies cell compartments. EMBO J **20:**2140-2151.

20. **Nisole S, Maroui MA, Mascle XH, Aubry M, Chelbi-Alix MK.** 2013. Differential Roles of PML Isoforms. Front Oncol **3:**125.

21. **Bernardi R, Pandolfi PP.** 2007. Structure, dynamics and functions of promyelocytic leukaemia nuclear bodies. Nat Rev Mol Cell Biol **8:**1006-1016.

22. **Geng Y, Monajembashi S, Shao A, Cui D, He W, Chen Z, Hemmerich P, Tang J.** 2012. Contribution of the C-terminal regions of promyelocytic leukemia protein (PML) isoforms II and V to PML nuclear body formation. J Biol Chem **287:**30729-30742.

23. **Li C, Peng Q, Wan X, Sun H, Tang J.** 2017. C-terminal motifs in promyelocytic leukemia protein isoforms critically regulate PML nuclear body formation. J Cell Sci **130:**3496-3506.

24. **Cuchet D, Sykes A, Nicolas A, Orr A, Murray J, Sirma H, Heeren J, Bartelt A, Everett RD.** 2011. PML isoforms I and II participate in PML-dependent restriction of HSV-1 replication. J Cell Sci **124:**280-291.

25. **Pomeranz LE, Reynolds AE, Hengartner CJ.** 2005. Molecular biology of

pseudorabies virus: impact on neurovirology and veterinary medicine. Microbiol Mol Biol Rev **69:**462-500.

26. **Parkinson J, Everett RD.** 2000. Alphaherpesvirus proteins related to herpes simplex virus type 1 ICP0 affect cellular structures and proteins. J Virol **74:**10006-10017.

27. **Everett RD, Boutell C, McNair C, Grant L, Orr A.** 2010. Comparison of the biological and biochemical activities of several members of the alphaherpesvirus ICP0 family of proteins. J Virol **84:**3476-3487.

28. **Zhang Q, Huang C, Yang Q, Gao L, Liu HC, Tang J, Feng WH.** 2016. MicroRNA-30c Modulates Type I IFN Responses To Facilitate Porcine Reproductive and Respiratory Syndrome Virus Infection by Targeting JAK1. J Immunol **196:**2272-2282.

29. **Takenouchi T, Suzuki S, Shinkai H, Tsukimoto M, Sato M, Uenishi H, Kitani H.** 2014. Extracellular ATP does not induce P2X7 receptor-dependent responses in cultured renal- and liver-derived swine macrophages. Results Immunol **4:**62-67.

30. **Xu A, Qin C, Lang Y, Wang M, Lin M, Li C, Zhang R, Tang J.** 2015. A simple and rapid approach to manipulate pseudorabies virus genome by CRISPR/Cas9 system. Biotechnol Lett **37:**1265-1272.

31. **Qin C, Zhang R, Lang Y, Shao A, Xu A, Feng W, Han J, Wang M, He W,**

Yu C, Tang J. 2019. Bclaf1 critically regulates the type I interferon response and is degraded by alphaherpesvirus US3. PLoS Pathog **15:**e1007559.

32. **Han J, Chadha P, Starkey JL, Wills JW.** 2012. Function of glycoprotein E of herpes simplex virus requires coordinated assembly of three tegument proteins on its cytoplasmic tail. Proc Natl Acad Sci U S A **109:**19798-19803.

33. **Zhang R, Xu A, Qin C, Zhang Q, Chen S, Lang Y, Wang M, Li C, Feng W, Zhang R, Jiang Z, Tang J.** 2017. Pseudorabies Virus dUTPase UL50 Induces Lysosomal Degradation of Type I Interferon Receptor 1 and Antagonizes the Alpha Interferon Response. J Virol **91**.

34. **Tang J, Wu S, Liu H, Stratt R, Barak OG, Shiekhattar R, Picketts DJ, Yang X.** 2004. A novel transcription regulatory complex containing death domain-associated protein and the ATR-X syndrome protein. J Biol Chem **279:**20369-20377.

35. **Bedell VM, Wang Y, Campbell JM, Poshusta TL, Starker CG, Krug RG, 2nd, Tan W, Penheiter SG, Ma AC, Leung AY, Fahrenkrug SC, Carlson DF, Voytas DF, Clark KJ, Essner JJ, Ekker SC.** 2012. In vivo genome editing using a high-efficiency TALEN system. Nature **491:**114-118.

36. **Condemine W, Takahashi Y, Zhu J, Puvion-Dutilleul F, Guegan S, Janin A, de The H.** 2006. Characterization of endogenous human promyelocytic leukemia isoforms. Cancer Res **66:**6192-6198.

613 37. **Gurrieri C, Capodieci P, Bernardi R, Scaglioni PP, Nafa K, Rush LJ,**
614 **Verbel DA, Cordon-Cardo C, Pandolfi PP.** 2004. Loss of the tumor
615 suppressor PML in human cancers of multiple histologic origins. J Natl
616 Cancer Inst **96:**269-279.
617 38. **Letunic I, Bork P.** 2018. 20 years of the SMART protein domain annotation
618 resource. Nucleic Acids Res **46:**D493-D496.
619 39. **Shen TH, Lin HK, Scaglioni PP, Yung TM, Pandolfi PP.** 2006. The
620 mechanisms of PML-nuclear body formation. Mol Cell **24:**331-339.
621 40. **Lallemand-Breitenbach V, de The H.** 2010. PML nuclear bodies. Cold
622 Spring Harb Perspect Biol **2:**a000661.
623 41. **Kamitani T, Kito K, Nguyen HP, Wada H, Fukuda-Kamitani T, Yeh ET.**
624 1998. Identification of three major sentrinization sites in PML. J Biol Chem
625 **273:**26675-26682.
626 42. **Muller S, Matunis MJ, Dejean A.** 1998. Conjugation with the ubiquitin-
627 related modifier SUMO-1 regulates the partitioning of PML within the
628 nucleus. EMBO J **17:**61-70.
629 43. **Sahin U, Ferhi O, Jeanne M, Benhenda S, Berthier C, Jollivet F, Niwa-**
630 **Kawakita M, Faklaris O, Setterblad N, de The H, Lallemand-**
631 **Breitenbach V.** 2014. Oxidative stress-induced assembly of PML nuclear
632 bodies controls sumoylation of partner proteins. J Cell Biol **204:**931-945.

633 44. **Laity JH, Lee BM, Wright PE.** 2001. Zinc finger proteins: new insights into
634 structural and functional diversity. Curr Opin Struct Biol **11:**39-46.
635 45. **Cuchet-Lourenco D, Boutell C, Lukashchuk V, Grant K, Sykes A,**
636 **Murray J, Orr A, Everett RD.** 2011. SUMO pathway dependent recruitment
637 of cellular repressors to herpes simplex virus type 1 genomes. PLoS Pathog
638 **7:**e1002123.
639 46. **Gu H, Zheng Y.** 2016. Role of ND10 nuclear bodies in the chromatin
640 repression of HSV-1. Virol J **13:**62.
641 47. **Lukashchuk V, Everett RD.** 2010. Regulation of ICP0-null mutant herpes
642 simplex virus type 1 infection by ND10 components ATRX and hDaxx. J
643 Virol **84:**4026-4040.
644 48. **Fogal V, Gostissa M, Sandy P, Zacchi P, Sternsdorf T, Jensen K,**
645 **Pandolfi PP, Will H, Schneider C, Del Sal G.** 2000. Regulation of p53
646 activity in nuclear bodies by a specific PML isoform. EMBO J **19:**6185-6195.
647 49. **Bischof O, Kirsh O, Pearson M, Itahana K, Pelicci PG, Dejean A.** 2002.
648 Deconstructing PML-induced premature senescence. EMBO J **21:**3358-
649 3369.

650 # FIGURES AND FIGURE LEGENDS

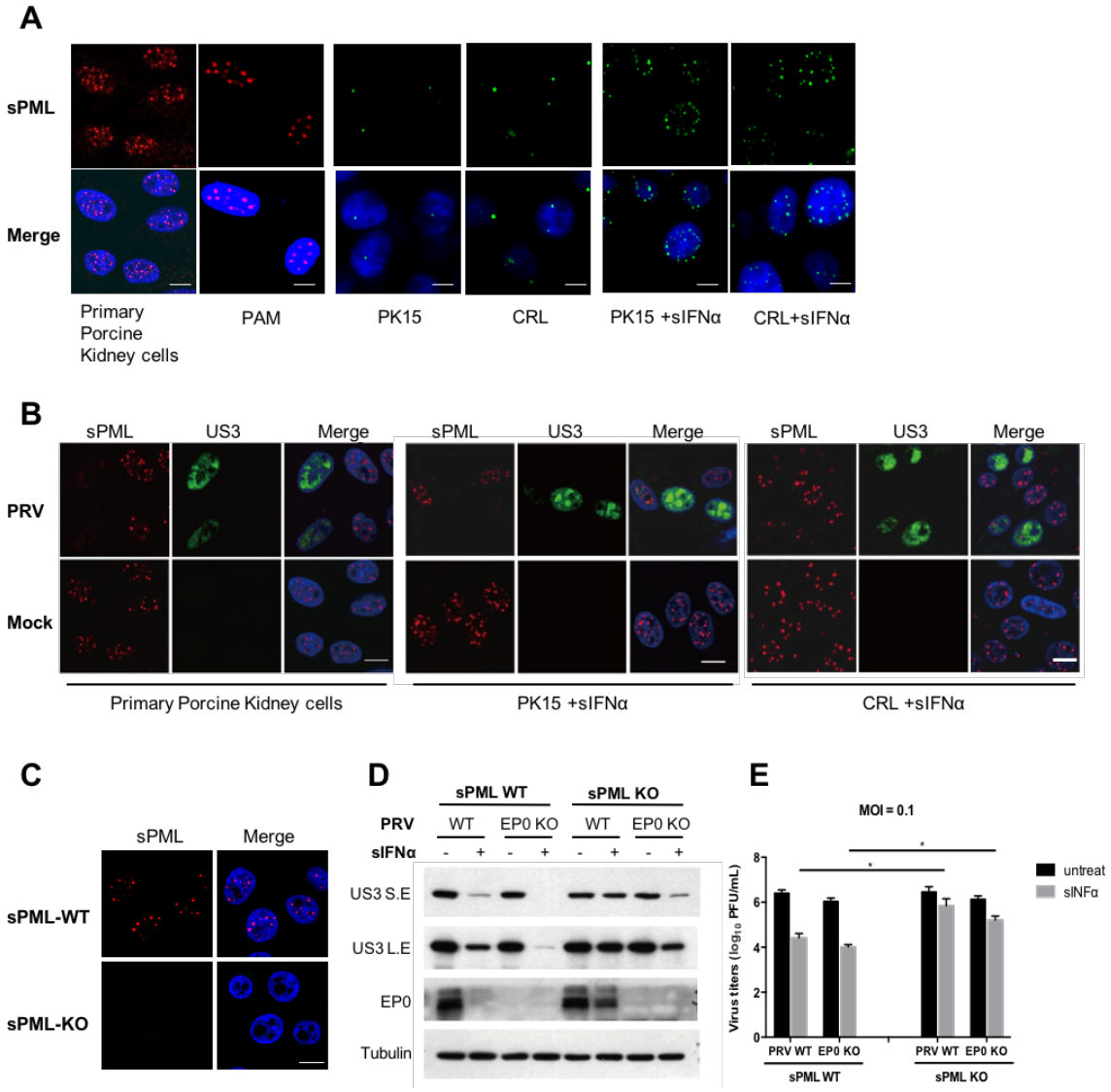

651 **Figure 1. Swine PML-NBs and their relationships with PRV infections.** (**A**)
652 Representative immunofluorescent images showing sPML-NBs in several types of
653 porcine cells, including freshly isolated primary porcine kidney cells and porcine
654 alveolar macrophages (PAM) (red, left panel), and cell lines PK15 and CRL without
655 or with 12 h of sIFNα pre-treatment (green, middle and right panels). The cells
656 were stained with an anti-sPML antibody, and the nuclei counterstained with DAPI

(blue). Scale bar is 5 μm. (**B**) Representative immunofluorescent images showing the disappearance of sPML-NBs (red) in PRV infected cells (US3 positive, green) as compared to un-infected cells (US3 negative). Primary porcine kidney cells (left), and PK15 (middle) and CRL cells (right) pre-treated with sIFNα were infected with PRV WT (MOI=1) and then stained with a rabbit anti-sPML, and a mouse anti-US3 primary antibody at 24 hpi. The nuclei were stained with DAPI (blue). Scale bar is 5 μm. (**C**) Immunofluorescent microscopy showing that sPML was knocked out in sPML-KO PK15 cells. sPML-WT and -KO PK15 cells were treated with sIFNα (500U/mL) for 12 h before immunostaining with an anti-sPML (red) antibody. The nuclei were stained with DAPI (blue). Scale bar is 5 μm. (**D and E**) Knockout of sPML increases PRV infection in PK15 cells pre-treated with sIFNα. Following treatments with PBS or sIFNα (500U/mL) for 12 h, sPML-WT and KO PK15 cells were infected with PRV-WT or PRV-EP0 KO (MOI=0.1) for 24 h. Cells were collected for western blot analysis of viral protein expressions using the indicated antibodies (D). Viruses released in supernatants were determined by plaque assay (E). Data are shown as mean ± SD of three independent experiments. Statistical analyses were performed by ANOVA, using GraphPad Prism software. *$p<0.05$.

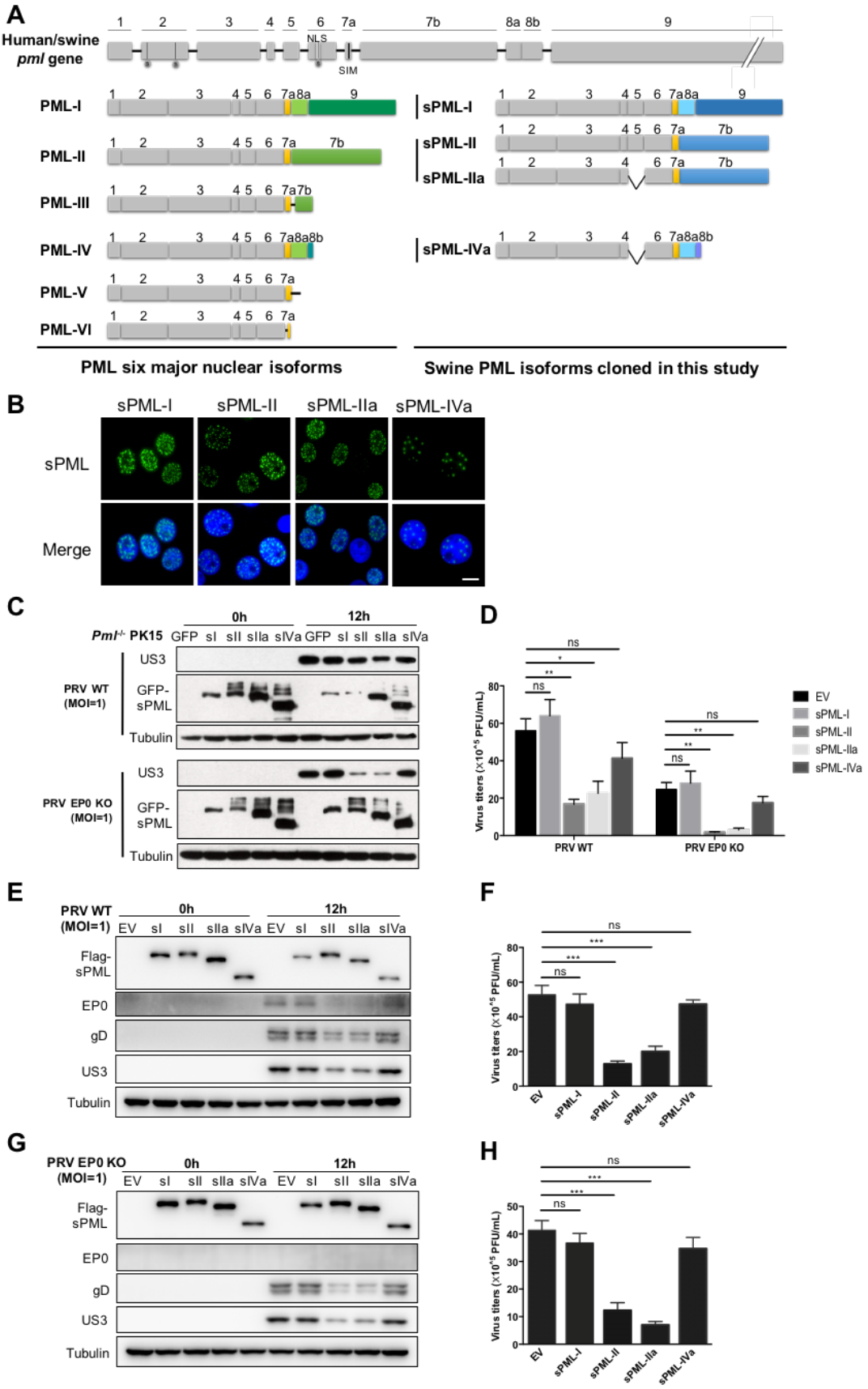

675 **Figure 2. sPML Isoform II/IIa not I and IVa restrict PRV infection.** (**A**) Schematic
676 diagrams of human/swine *pml* gene, the six major nuclear isoforms of human PML
677 and likely swine PML (sPML), and the four sPML isoforms cloned in this study. S:
678 SUMO modification, NLS: nuclear location sequence, SIM: SUMO Non-covalent
679 interaction motif. (**B**) Green fluorescent protein (GFP) fluorescence analysis of
680 sPML-NBs in sPML-KO PK15 cells stably expressing GFP-tagged sPML isoforms
681 as indicated. The nuclei were counterstained with DAPI (blue). Scale bar is 5 μm.
682 (**C and D**) sPML-KO PK15 cells stably expressing GFP or GFP-tagged sPML
683 isoforms (sI, sII, sIIa or sIVa) were infected with PRV-WT (MOI=1) or PRV-EP0 KO
684 (MOI=1) for 12 h. Western blotting analyzed US3, GFP-sPML and α-tubulin
685 expression in cell lysates (C). Plaque assay analyzed virus titers in supernatants
686 (D). (**E-H**) sPML-WT PK15 cells transfected with Flag-tagged sPML-I, sPML-II,
687 sPML-IIa, or sPML-IVa expressing plasmids were infected with PRV-WT (MOI=1)
688 (E and F) or PRV-EP0 KO (MOI=1) (G and H) for 12 h. Western blotting analyzed
689 Flag-sPML, EP0, gD, US3 and α-tubulin expression in cell lysates (E and G).
690 Plaque assay analyzed virus titers in supernatants (F and H). Data are shown as
691 mean ± SD of three independent experiments. Statistical analyses were performed
692 by ANOVA, using GraphPad Prism software. *p<0.05; **p<0.01; ***p<0.001.

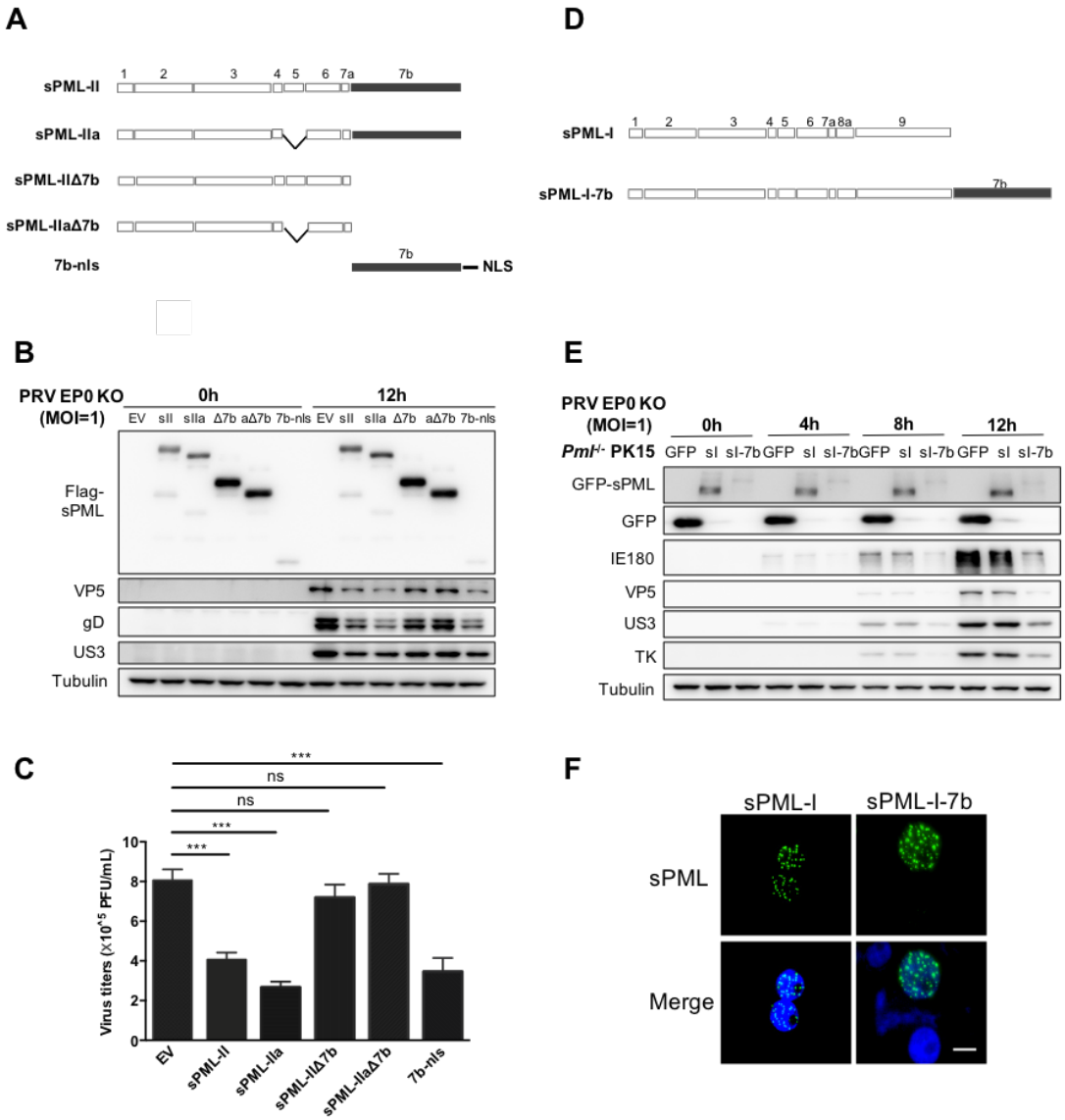

Figure 3. The unique C-terminal region encoded by exon 7b of sPML-II/-IIa possesses an anti-PRV activity. (**A**) Schematic representations of sPML-II/sPML-IIa, 7b deletion mutants sPML-IIΔ7b/sPML-IIaΔ7b, and the nuclear targeting 7b fragment 7b-nls. (**B and C**) 7b region of sPML-II/-IIa possesses an anti-PRV activity. sPML-WT PK15 cells transfected with Flag-sPML-II, -sPML-IIa, -sPML-IIΔ7b (Δ7b), -sPML-IIaΔ7b (aΔ7b) or -7b-nls expressing plasmids were

700 infected with PRV-EP0 KO (MOI=1) for 12 h. Cells were collected for western blot
701 analysis of viral protein expressions using the indicated antibodies (B). Viruses
702 released in supernatants were determined by plaque assay (C). (**D**) Schematic
703 representations of sPML-I and sPML-I-7b in which 7b was fused to the C-terminal
704 end of sPML-I. (**E**) sPML-KO PK15 cells stably expressing the indicated proteins
705 were infected with PRV-EP0 KO (MOI=1) for 4, 8, 12 h. Western blotting analyzed
706 GFP-sPML, GFP, IE180, VP5, US3, TK and α-tubulin expression. (**F**) GFP
707 fluorescence analysis of sPML-NBs in sPML-KO PK15 cells stably expressing
708 GFP-tagged sPML-I or sPML-I-7b. The nuclei were counterstained with DAPI
709 (blue). Scale bar is 5 μm. Data are shown as mean ± SD of three independent
710 experiments. Statistical analyses were performed by ANOVA, using GraphPad
711 Prism software. ***p<0.001.

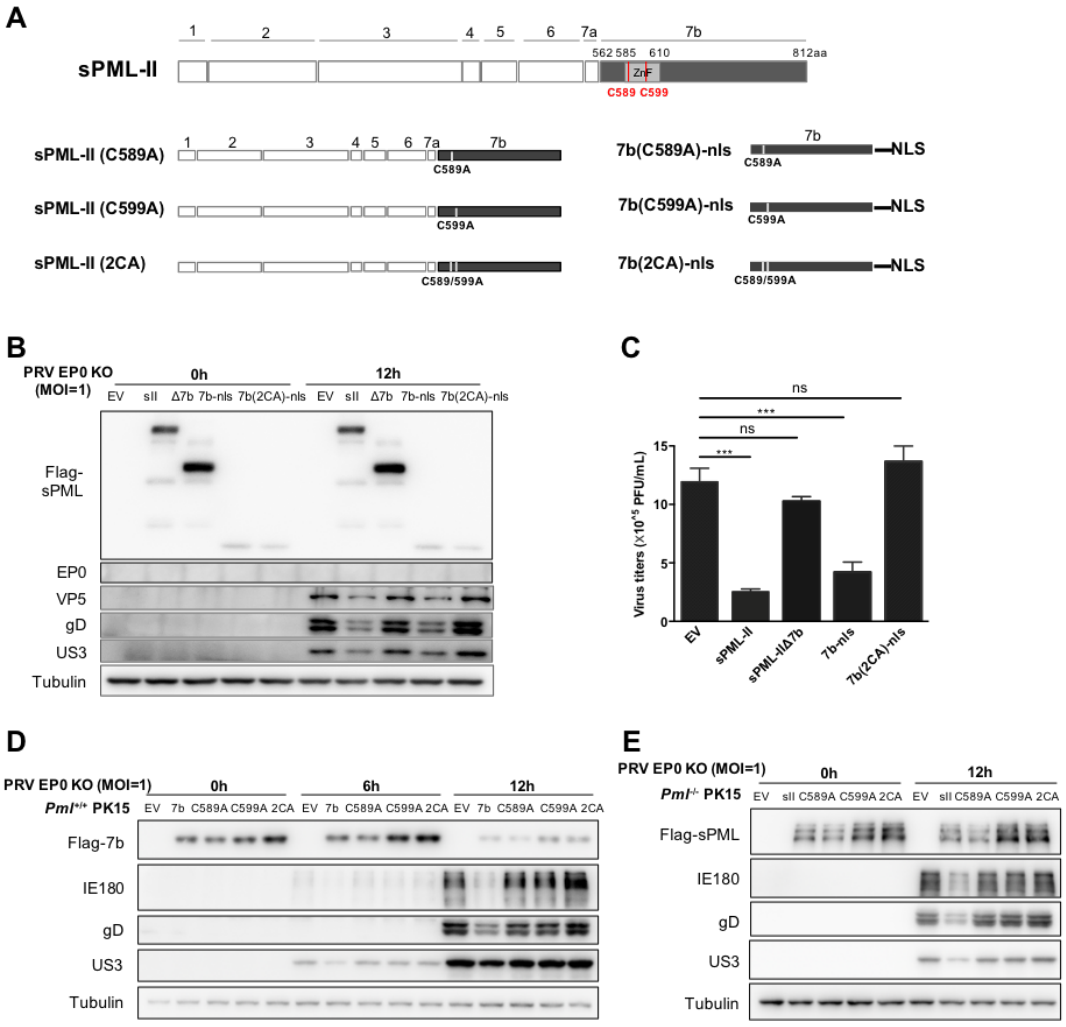

Figure 4. Cysteine residue 589 and 599 in 7b contribute to the anti-PRV activity of 7b and sPML-II/IIa. (**A**) Schematics showing the predicted zinc finger region in 7b using SMART and the mutants used in this study with one or both cysteine residue(s) changed to alanine (**B and C**) sPML-WT PK15 cells expressing sPML-II, or the indicated mutants were infected with PRV-EP0 KO (MOI=1) for 12 h, followed by western blotting (B) and plaque assay (C) as above described. (**D and E**) sPML-WT PK15 cells stably expressing Flag-7b-nls, -7b(C589A)-nls, -7b(C599A)-nls or -7b(2CA)-nls (D) or sPML-KO PK15 cells stably expressing Flag-

721 sPML-II, -II(C589A), -II(C599A) or -II(2CA) (E) were infected with PRV-EP0 KO
722 (MOI=1) and analyzed by Western blotting. Data are shown as mean ± SD of three
723 independent experiments. Statistical analyses were performed by ANOVA, using
724 GraphPad Prism software. ***p<0.001.

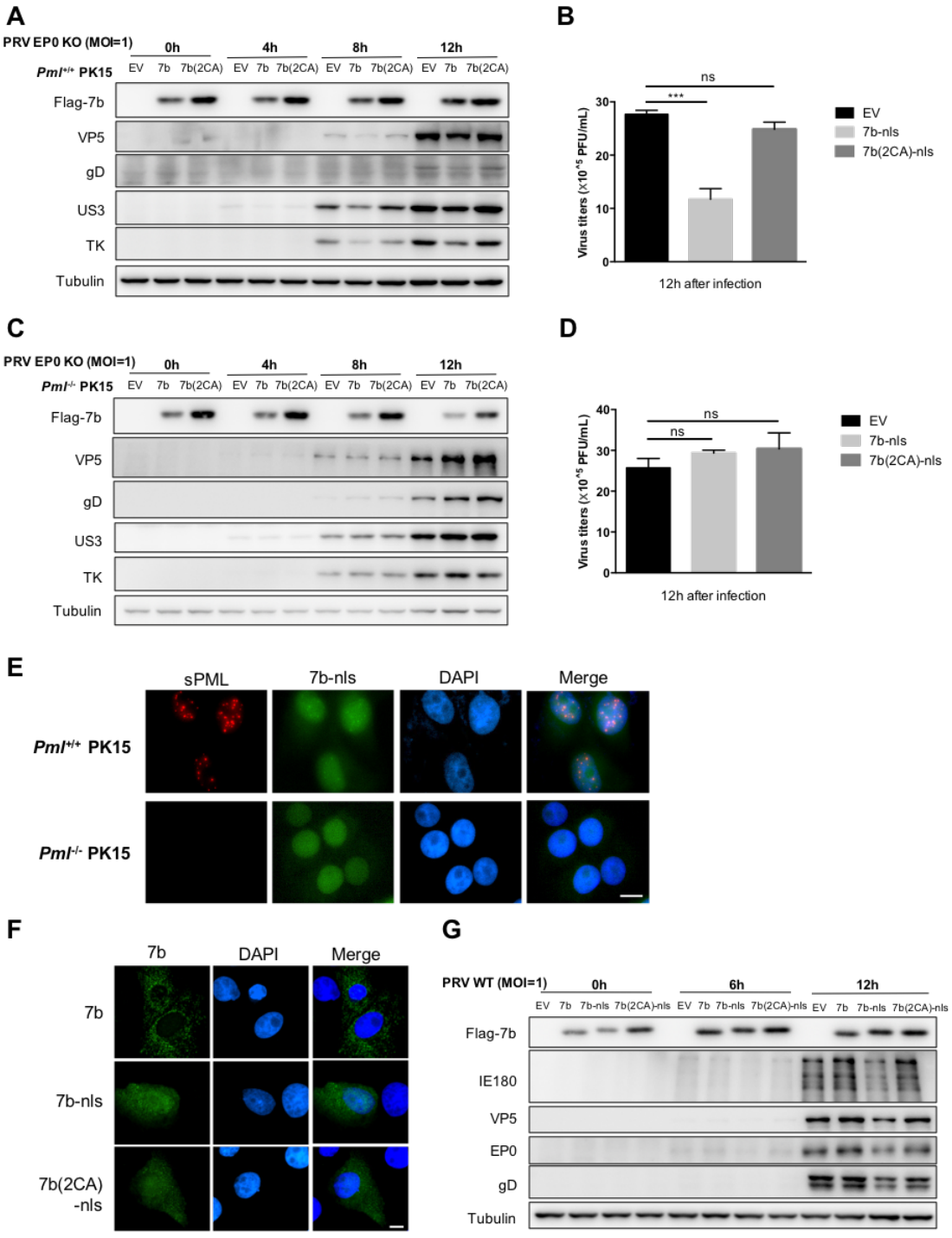

Figure 5. 7b mediated inhibition of PRV infection depends on its localization in sPML-NB. (**A-D**) 7b exhibits PRV inhibition in sPML-WT, but not in -KO cells. sPML-WT (A and B) or -KO PK15 (C and D) cells stably expressing Flag-7b-nls or

729 -7b(2CA)-nls were infected with PRV-EP0 KO (MOI=1) for 4, 8 and 12 h, followed
730 by western blot analysis of the cells for viral protein expressions using the indicated
731 antibodies (A and C), and plaque assay of the virus particles released in the
732 supernatants (B and D). (**E**) Representative immunofluorescent images showing
733 the colocalization of 7b (green) and endogenous sPML-NBs (red) in sPML-WT
734 PK15 cells. sPML-WT and -KO PK15 cells stably expressing Flag-tagged 7b-nls
735 were treated with sIFNα (500U/mL) for 12 h before immunostaining with an anti-
736 sPML (red) and anti-Flag (green) antibodies. The nuclei were counterstained with
737 DAPI (blue). Scale bar is 5 μm. (**F**) Representative immunofluorescent images
738 showing that 7b without NLS localizes in the cytoplasm. sPML-WT PK15 cells
739 transfected with Flag-7b, -7b-nls or -7b(2CA)-nls expressing plasmids were
740 analyzed by immunofluorescence microscopy using anti-Flag (green) antibody.
741 The nuclei were counterstained with DAPI (blue). Scale bar is 5 μm. (**G**) 7b without
742 NLS losses the ability to inhibit PRV. sPML-WT PK15 cells transfected with the
743 indicated plasmids were infected with PRV-WT (MOI=1) for 6 and 12 h, followed
744 by western blotting analyzed using the indicated antibodies. Data are shown as
745 mean ± SD of three independent experiments. Statistical analyses were performed
746 by ANOVA, using GraphPad Prism software. ***$p<0.001$.

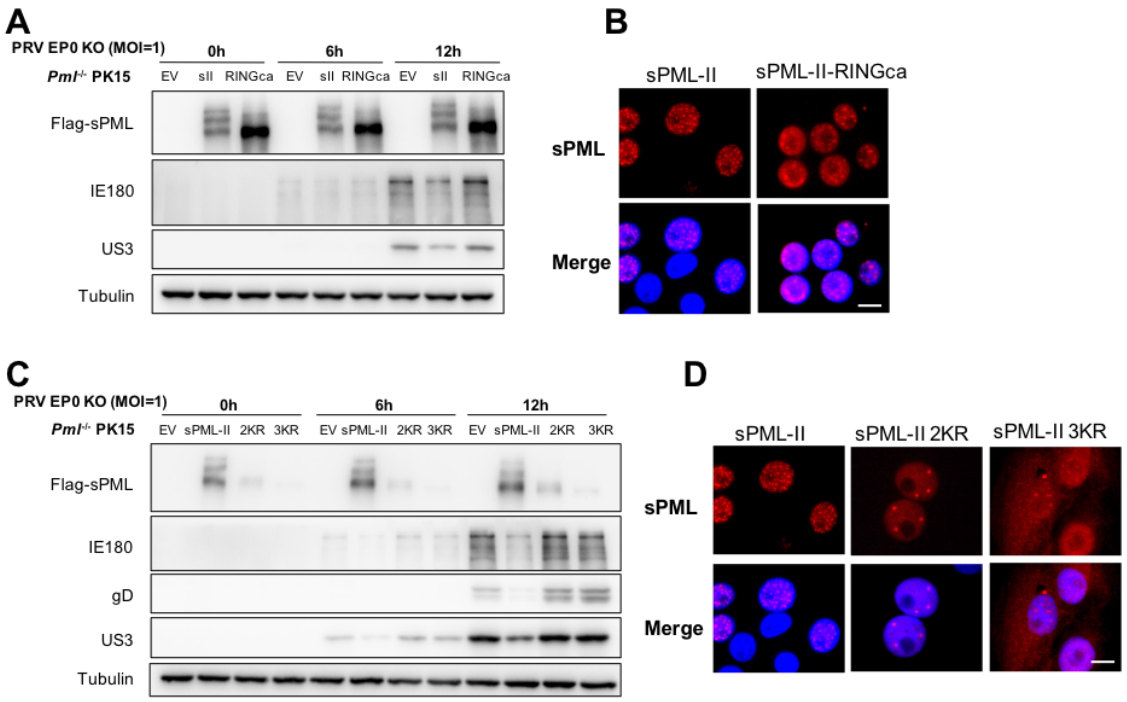

Figure 6. sPML-II inhibits PRV dependently on the normal formation of sPML-NBs. (**A and B**) The RING finger domain is required for sPML-II to inhibit PRV. sPML-KO PK15 cells stably expressing Flag-sPML-II or -sPML-II-RINGca were either infected with PRV-EP0 KO (MOI=1) for 6 and 12 h, followed by western blot analysis using the indicated antibodies (A), or immuno-stained with an anti-Flag (red) antibody followed by immunofluorescence microscopy (B). The nuclei were counterstained with DAPI (blue). Scale bar is 5 μm. (**C and D**) Lysine residues 65, 160 and 482 contribute to the anti-PRV activity of sPML-II. sPML-KO PK15 cells stably expressing Flag-sPML-II, -sPML-II 2KR (K65/160R) or -sPML-II 3KR (K65/160/482R) were either infected with PRV-EP0 KO (MOI=1) for 6 and 12 h, followed by western blot analysis using the indicated antibodies (C), or immuno-stained with an anti-Flag (red) antibody followed by immunofluorescence

760 microscopy (D). The nuclei were counterstained with DAPI (blue). Scale bar is 5

761 μm.

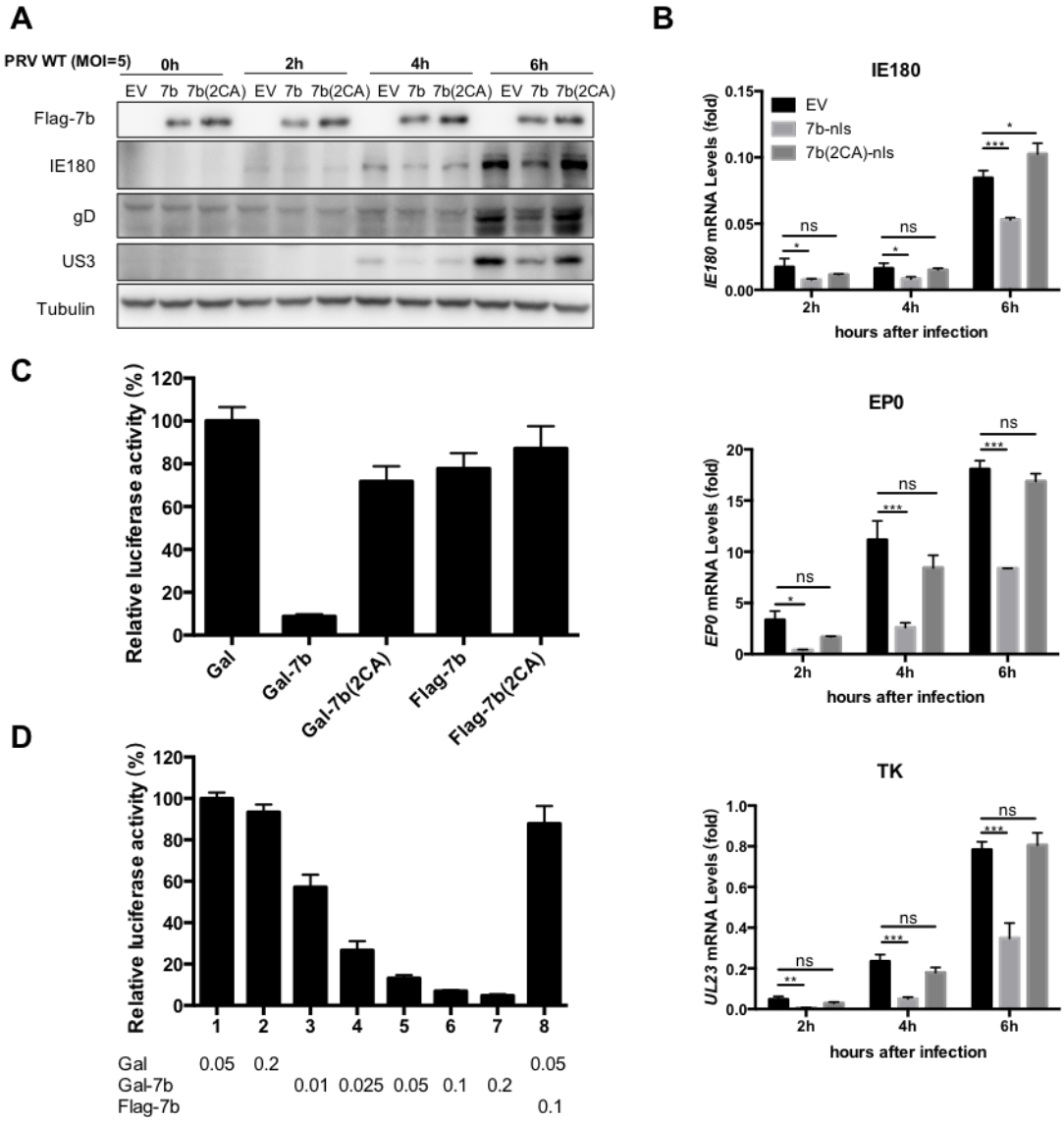

Figure 7. sPML exon 7b function as a transcription repressor. (**A and B**) 7b inhibits viral gene transcriptions during PRV infection. sPML-WT PK15 cells transfected with Flag-7b-nls or -7b(2CA)-nls expressing plasmids were infected with PRV-WT (MOI=5) for 2, 4 and 6 h, followed by western blotting analysis of Flag-7b, IE180, gD, US3 and α-tubulin expression (A), or qRT-PCR analysis of *IE180, EP0* and *UL23* mRNAs (B). (**C and D**) Transcriptional repression by Gal-

7b. HEK293T cells were transfected with plasmids expressing Gal, Gal-7b or controls as indicated (C) or with the increased amounts (in micrograms) of Gal or Gal-7b as indicated (D) together with 5xGal-TK-luciferase reporter and CMV-β-galactosidase plasmids. Luciferase activities were normalized with β-galactosidase expression and then compared with that of 50 ng of Gal transfected groups which were arbitrarily set as 100%. Data are shown as mean ± SD of three independent experiments. Statistical analyses were performed by ANOVA, using GraphPad Prism software. *$p<0.05$; **$p<0.01$; ***$p<0.001$.

777 **TABLE 1** Primers used for sPML isoforms and their mutants cloning

Primer(restriction enzyme site)	Sequence (5'-3')
pSin-F-sPMLs-F (ECORI)	ACGATGACGACAAGGAATTC ATGCAGCAGGAACCGGCA
pSin-F-GFP-sPMLs-F	ATGGACGAGCTGTACAAGGGTGGC ATGCAGCAGGAACCGGCA
pSin-sPML-I-R (SpeI)	TGCGGATCCTTCGAACTAGT TCAGCTCTCCTGGGAAGC
pSin-sPML-II-R (SpeI)	TGCGGATCCTTCGAACTAGT TTAGAGGCTTGTCTGCGG
pSin-sPML-IIa-R (SpeI)	TGCGGATCCTTCGAACTAGT TTAGAGGCTTGTCTGCGG
pSin-sPML-IVa-R (SpeI)	TGCGGATCCTTCGAACTAGT TCAGGGACTAAGGTAGAA
pRK5-F-sPMLs-F (BamHI)	GACGATGACAAGGGATCC ATGCAGCAGGAACCGGCA
pRK5-F-sPML-I-R (HindIII)	GCCATGGCGGCCAAGCTT TCAGCTCTCCTGGGAAGC
pRK5-F-sPML-II-R (HindIII)	GCCATGGCGGCCAAGCTT TTAGAGGCTTGTCTGCGG
pRK5-F-sPML-IIa-R (HindIII)	GCCATGGCGGCCAAGCTT TTAGAGGCTTGTCTGCGG
pRK5-F-sPML-IVa-R (HindIII)	GCCATGGCGGCCAAGCTT TCAGGGACTAAGGTAGAA
pRK5-F-sPML-II/IIaΔ7b -R (HindIII)	GCCATGGCGGCCAAGCTT TTAACACGAGTTTTCAGCATC
pRK5-F-7b-nls-F (BamHI)	GACGATGACAAGGGATCC ATGGCGGAGCCCATGGAG
pRK5-F-7b-nls-R (HindIII)	GCCATGGCGGCCAAGCTTTTAGACCTTCCGCTTCTTCTTTGGG CCACCGAGGCTTGTCTGCGGGGT
pRK5-F-7b-R (HindIII)	GCCATGGCGGCCAAGCTT TTAGAGGCTTGTCTGCGG
pSin-F-7b-nls-F (ECORI)	ACGATGACGACAAGGAATTC ATGGCGGAGCCCATGGAG
pSin-F-7b-nls-R (SpeI)	TGCGGATCCTTCGAACTAGT TTAGACCTTCCGCTTCTT
pSin-sPML-I-R (7b)	CTCCATGGGCTCCGCCATGCCACCGCTCTCCTGGGAAGCCCT
pSin-7b-F (sPML-I)	AGGGCTTCCCAGGAGAGCGGTGGCATGGCGGAGCCCATGGAG
pSin-7b-R (SpeI)	TGCGGATCCTTCGAACTAGT TTAGAGGCTTGTCTGCGG
7b-F (C589A)	TCCCGCCCCGCCCGGGCCTT

7b-R (C589A)	AAGGCCCGGGCGGGGCGGGA
7b-F (C599A)	GTGGTACAGCCCGCTTCCAA
7b-R (C599A)	TTGGAAGCGGGCTGTACCAC
sPML-II (K65R)-F	AAGGAAGCCAGATGCCCCAAG
sPML-II (K65R)-R	CTTGGGGCATCTGGCTTCCTT
sPML-II (K160R)-F	TGGTTCCTCAGGCACGAGGCC
sPML-II (K160R)-R	GGCCTCGTGCCTGAGGAACCA
sPML-II (K482R)-F	AAGGTCATCAGGATGGAGTCA
sPML-II (K482R)-R	TGACTCCATCCTGATGACCTT
sPML-II RING (C88/91A)-F	CCGCAGCCGGGCTTGCAGGCCCCCATCGCCCAGGCACCCTGG
sPML-II RING (C72/77/80A)-F	AAGCTGCTACCTGCTCTGCACACGCTGGCTTCAGGAGCCCTGC CGCAGCCGGGCTTG
sPML-II RING (C57/60A)-F	CAGTTCTTGCGCGCCCAGGGCGCCCGGAAGGAAGCCAAATGC CCCAAGCTGCTACCTGCT
sPML-II RING (C57/60A)-R	AGCAGGTAGCAGCTTGGGGCATTTGGCTTCCTTCCGGGCGCC CTGGGCGCGCAAGAACTG